Progress In Electromagnetics Research M, Vol. 95, 125–133, 2020

Sensitivity Considerations for Inline Fully Canonical Filters at Ku-Band

Jordi Verdú Tirado[1, *], Ivan Baro[2], Eloi Guerrero[1], Patricia Silveira[1], Ángel Triano[1], Gary Junkin[1], and Pedro de Paco[1]

Abstract—In this paper, a planar inline fully-canonical topology is proposed to reduce sensitivity to fabrication tolerances compared to conventional inline all-pole configurations. Major concerns are related with errors in the absolute positioning of via-holes to ground which affect inter-resonator (main-line) couplings. The total expanded sensitivity considering variations of the main-line couplings have been obtained for fully and non-fully canonical configurations. The result shows that sensitivity is lower in the case of fully-canonical topologies. Moreover, the allocation of the transmission zeros plays a key role in terms of sensitivity. A prototype has been designed for the Ku-band based on asymmetrical coupled lines obtaining IL = -1.6 dB, RL below -18 dB, and out-of-band rejection higher than -50 dB.

1. INTRODUCTION

Planar technologies are considered for Ku-band filters in space applications as an alternative to coupled waveguide cavities in order to reduce the size and weight of transceiver units [1]. In particular, microstrip filter designs using classical and cross-coupled hairpin, interdigital or slowave resonators in the Ku-band are found in [2]. These inline canonical filters are very well-known topologies in which a set of resonant nodes (RNs) are connected by means of main-line couplings. When no cross-couplings are present, non-fully-canonical (NFC) all-pole filters can be obtained which are characterized by the allocation of all the transmission zeros (TZ) at infinity.

One of the drawbacks of these NFC configurations is the high sensitivity to fabrication tolerances, so small fabrication deviations can lead to out of specification filter responses mainly in what refers to return loss. This is more critical in configurations requiring short-circuited (SC) terminations since they are particularly dependent on the fabrication tolerances of the absolute positioning of the via-holes on the board [3, 4].

With the objective to reduce the sensitivity to fabrication tolerances, an inline fully-canonical (FC) filter based on extracted pole sections is considered. In this case, the filtering function contains as many finite transmission zeros as the order of the filter N. Although it is mentioned that FC are less sensitive to fabrication tolerances since each transmission zero is independently controlled [5], a detailed analysis is provided in this work based on the total expanded sensitivity considering different configurations. It will also be proven that the allocation of the finite transmission zeros plays an important role in terms of sensitivity.

To provide an experimental validation, an FC filter based on asymmetrical coupled lines [6, 7] is proposed, as an alternative to classical coupled resonator configurations. As it will be further discussed, the equivalences between the nodal representation of the extracted pole FC filter, the distributed model, and the prototype based on asymmetrical coupled lines are outlined in Fig. 1. The filter has been designed to operate in the Ku-band, with $f_0 = 13.55$ GHz.

Received 1 July 2020, Accepted 23 July 2020, Scheduled 17 August 2020

* Corresponding author: Jordi Verdú Tirado (jordi.verdu@uab.cat).

[1] Telecommunications and Systems Engineering Department, Universitat Autònoma de Barcelona (UAB), Spain. [2] Sener Aerospacial, Spain.

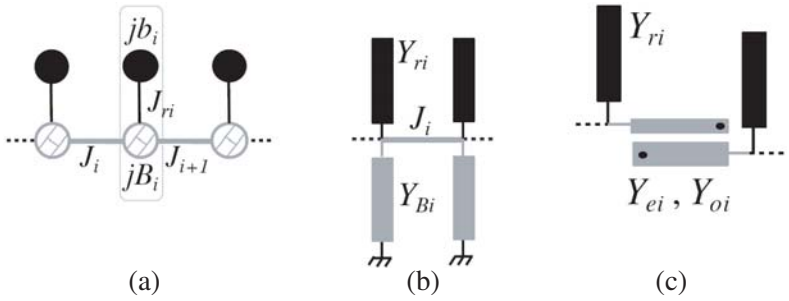

Figure 1. (a) Nodal topology, (b) Distributed transmission lines equivalent and (c) Asymmetric transmission lines equivalent.

The paper begins by analysing the total extended sensitivity in both FC and NFC configurations. Subsequently, the equivalence using the asymmetrical coupled lines is briefly discussed. Finally, the planar FC filter in Ku-band is designed, fabricated, and experimentally validated, and favourable conclusions are presented.

2. SENSITIVITY ANALYSIS FOR FULLY-CANONICAL AND NON-FULLY-CANONICAL ALL-POLE FILTERS

The nodal representation for an inline FC filter is depicted in Fig. 1(a). This is composed by the connection of basic cells, the dangling resonator, defined in the lowpass domain by the non-resonant node (NRN) reactance jB_i, the resonant node (RN) susceptance jb_i, and the coupling J_{ri} between the RN and NRN. The dangling resonators are connected by means of main-line couplings J_{ij} [8]. Following the minimum path rule [9], since there is a direct source-to-load coupling through the NRNs path, the FC topology may present as many TZs as the order of the filter N.

The use of synthesis tools allows obtention of the coupling matrix $[M]$ for both NFC and FC filters [8, 10], defined by the filter function. In the case of NFC topologies, the RNs are allocated in the diagonal of $[M]$, while the couplings and cross-couplings, if they exist, are in the off-diagonal positions. In the case of the FC configuration, the difference is that the NRN reactances are allocated in the diagonal of $[M]$. However, they are not frequency dependent. Therefore, corresponding positions in the frequency matrix $[W]$ will be null. For FC case, main-line couplings are those connecting NRNs. Taking into account that termination (source and load) nodes are allocated in positions (1, 1) and (2, 2), respectively, $[M]$ and $[W]$ matrices are defined as follows,

$$M=\begin{pmatrix} jB_s & 0 & 0 & 0 & 0 & J_{S1} & 0 & 0 & \cdots \\ 0 & jB_L & 0 & 0 & 0 & 0 & 0 & 0 & \cdots \\ 0 & 0 & -jb_1 & 0 & 0 & J_{r1} & 0 & 0 & \cdots \\ 0 & 0 & 0 & -jb_2 & 0 & 0 & J_{r2} & 0 & \cdots \\ 0 & 0 & 0 & 0 & \ddots & 0 & 0 & \ddots & \cdots \\ J_{S1} & 0 & J_{r1} & 0 & 0 & jB_1 & J_{12} & 0 & \cdots \\ 0 & 0 & 0 & J_{r2} & 0 & J_{12} & jB_2 & J_{23} & \cdots \\ 0 & 0 & 0 & 0 & \ddots & 0 & J_{23} & \ddots & \cdots \end{pmatrix} \quad W=\begin{pmatrix} 0 & 0 & 0 & 0 & 0 & 0 & 0 & 0 & \cdots \\ 0 & 0 & 0 & 0 & 0 & 0 & 0 & 0 & \cdots \\ 0 & 0 & 1 & 0 & 0 & 0 & 0 & 0 & \cdots \\ 0 & 0 & 0 & 1 & 0 & 0 & 0 & 0 & \cdots \\ 0 & 0 & 0 & 0 & \ddots & 0 & 0 & 0 & \cdots \\ 0 & 0 & 0 & 0 & 0 & 0 & 0 & 0 & \cdots \\ 0 & 0 & 0 & 0 & 0 & 0 & 0 & 0 & \cdots \\ 0 & 0 & 0 & 0 & 0 & 0 & 0 & \ddots & \cdots \end{pmatrix} \tag{1}$$

Since there is a direct link between the coupling matrix and physical dimensions of the filter, the filter sensitivity can be evaluated by the gradient of S_{11} with respect to $[M]$-entries. For high variations on ΔM_{ij} it is more accurate to use the expanded sensitivity $K_{ij,EXT}$ [11]. This can be calculated, at each frequency point, as the highest value given a certain interval in ΔM_{ij} :

$$K_{ij,EXT} = \max\left(\left|\frac{\partial S_{11}}{\partial M_{ij}}\right|_{M_{ij,\min}<M_{ij}<M_{ij,\max}}\right) \tag{2}$$

The main fabrication issues are related to the positioning of the via-holes affecting inter-resonator (main-line) couplings, that is, M_{ij} elements connecting RNs in the NFC configuration and NRNs in the FC one. For the analysis of the total expanded sensitivity and taking into account the tolerances related to the fabrication process, variations of $\Delta M_{ij} = \pm 0.055$ have been considered.

First, the total expanded sensitivity has been obtained for an all-pole NFC configuration with RL = 15 dB and different filter orders ranging from $N = 4, \ldots, 11$. As shown in Fig. 2, higher order leads to higher sensitivity in the in-band region. On the other hand, as the order increases, so the selectivity, and the sensitivity drops faster in the transition from the in-band to the out-of-band region ($|\Omega| > 1$), with Ω being the normalized frequency. The observed peaks in the total expanded sensitivity corresponds to the position of the reflection zeros. Then, for odd configurations in which there is a reflection zero allocated at $\Omega = 0$ rad/s, a local maximum will be present. It has to be pointed out that there is a direct relationship between the total expanded sensitivity and the total average stored energy (TASE) in such a way that at the position of the reflection zeros, the local maximum value and the TASE are coincident [11, 12].

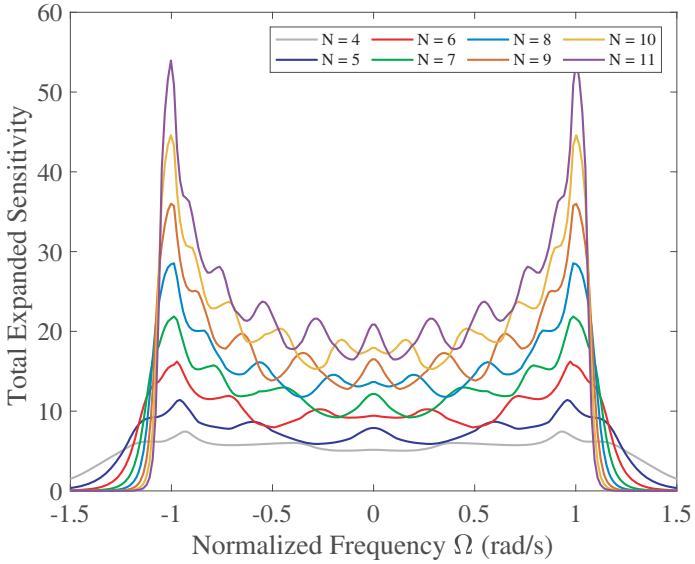

Figure 2. Total expanded sensitivity $K_{ij,EXT}$ for NFC all-pole configuration with $N = 4, \ldots, 11$; RL = 15 dB $\Delta M_{ij} = \pm 0.055$.

Taking into account the results for the all-pole configurations, several considerations must be taken into account in order to analyse the FC extracted pole. In FC, the allocation of the reflection zeros is symmetric with respect $\Omega = 0$ rad/s as it is the total expanded sensitivity. In FC configurations, the allocation of the reflection zeros may not be symmetric, and there is a strong relation with the allocation of the finite transmission zeros. Due to this, it is worthy to differentiate between even and odd configurations.

Figure 3 shows the total expanded sensitivity for even and odd FC extracted pole configurations. Without loss of generality, the finite transmission zeros have been allocated at alternating $\Omega_i = \pm 3.2$ rad/s. As it occurs in the all-pole case, for even and odd configurations, as the order of the filter increases, the in-band sensitivity also increases. The result for the even configuration in Fig. 3(a) shows a symmetric behaviour of the total expanded sensitivity in the transition region between the in-band and out-of-band. In the case of odd configurations, the multiplicity of the transmission zero above the passband, that is $\Omega = +3.2$ rad/s, is one degree higher. This effect can be observed in Fig. 3(b), where the total expanded sensitivity drops faster above the passband than below since the selectivity is higher in this region. Unlike the all-pole, in FC configurations, reflection zeros (RZ) are usually asymmetrically allocated in the in-band.

With the aim to observe how the allocation of the finite transmission zeros affects the total expanded

sensitivity, two FC extracted pole configurations with $N = 4$ and $N = 10$ and position of the finite transmission zero at $\Omega = \pm 3.2$ rad/s (solid lines) and $\Omega = \pm 1.2$ rad/s (dashed lines) have been compared as shown in Fig. 4. In what refers to the drop of the sensitivity, it is evident that this is faster in the case where the transmission zero is closer to the bandpass since the selectivity will be higher.

The in-band behavior in both cases is also different. As discussed in [13], the filter's sensitivity depends on the frequency separation between reflection zeros. The lower the frequency distance is between zeros, the higher the sensitivity is. This effect is more evident for even configurations where a

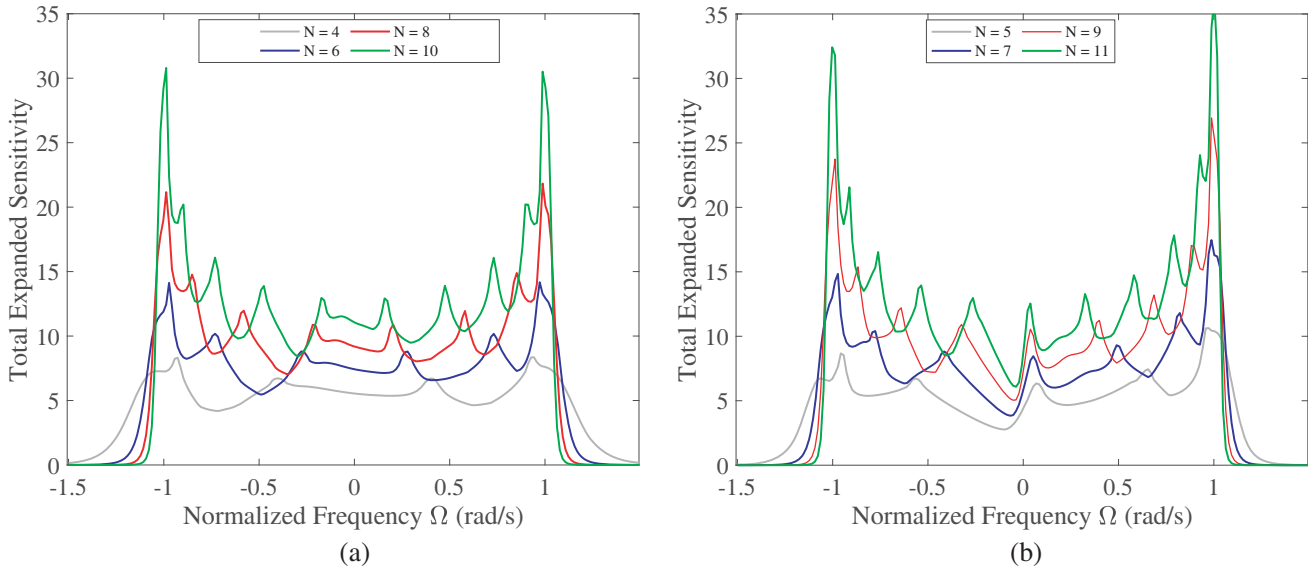

Figure 3. Comparison for (a) even, and (b) odd configurations. The transmission zeros are allocated at $\Omega_i = \pm 3.2$ rad/s. (a) Comparison for even configurations with $N = 4$, 6, 8, 10. (b) Comparison for odd configurations with $N = 5$, 7, 9, 11.

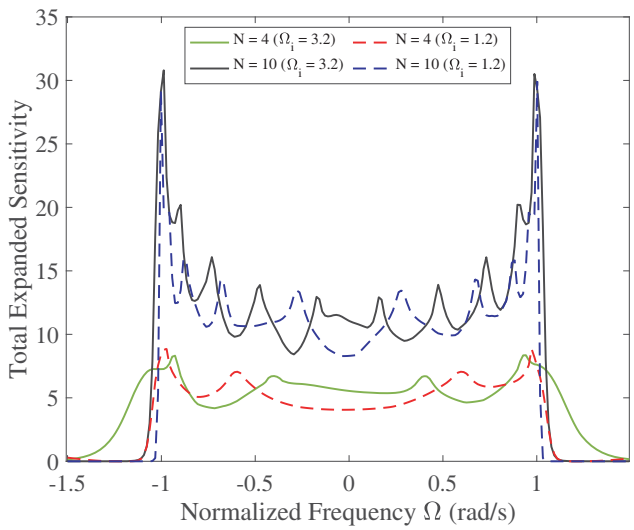

Figure 4. Comparison of the total expanded sensitivity for FC extracted pole filters with $N = 4$ and $N = 10$; RL = 15 dB and finite transmission zeros at $\Omega = \pm 3.2$ (solid lines) and $\Omega = \pm 1.2$ (dashed lines).

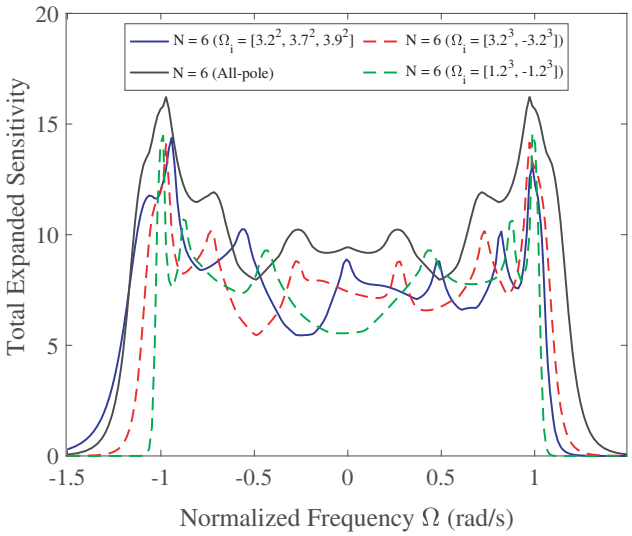

Figure 5. Comparison of the total expanded sensitivity for an all-pole $N = 6$ filter, and FC extracted pole configurations with $N = 6$ and different distribution of finite transmission zeros.

pair of reflection zeros are allocated almost symmetrically around the centre of the bandpass $\Omega = 0\,\text{rad/s}$ unlike the odd case. On the other hand, the finite transmission zeros are responsible for the allocation of the reflection zeros. As seen in Fig. 4, as the transmission zero is closer to the bandpass, the reflection zeros tend to be also allocated close to the bandpass edge. The fact of increasing the distance between reflection zeros leads to decreasing the sensitivity in the centre of the band, minimizing return loss degradation in this region.

As it will be further discussed in the next section, the proposed prototype can be only designed in such a way that all the transmission zeros are allocated above the passband. Taking this into consideration, it is worthy to carry out a comparison between an all-pole NFC and the FC extracted pole with the transmission zeros at $\Omega = 3.2\,\text{rad/s}$, $\Omega = 3.7\,\text{rad/s}$, and $\Omega = 3.9\,\text{rad/s}$, each with multiplicity 2. Previous configurations with transmission zeros above and below the passband have also been included in the comparison. The results are shown in Fig. 5. First, it can be seen that the all-pole configuration is the most sensitive. The prototype to be designed will contain all TZs above the passband ($\Omega_i > +1$); therefore, the sensitivity above the passband will drop fast. On the other hand, since no TZs are below the passband, the sensitivity in this region will be comparable to that of the all-pole configuration. In relation with the FC with alternating sign transmission zeros, the sensitivity in the centre of the band is lower in the case of the configuration with the highest selectivity ($\Omega = \pm 1.2\,\text{rad/s}$. As previously discussed, the allocation of the local maximum corresponds to the position of the reflection zeros.

3. INLINE FULLY-CANONICAL FILTER DESIGN BASED ON ASYMMETRIC COUPLED LINES

An in-line fully canonical extracted pole filter is proposed as an alternative to the classical coupled resonator filter in order to improve sensitivity to fabrication tolerances. As previously mentioned, the prototype will be implemented in planar technology by means of asymmetric coupled lines (ACL) sections. To design the filter, first of all, the characteristic polynomials are obtained once the order of the filter N, RL, and the allocation of TZs are set [9]. The elements are obtained by means of successive extractions from the input admittance, or equivalently by successive updates of the $[ABCD]$ matrix as proposed in [8]. At this point, the elements of the lowpass prototype corresponding to the nodal representation in Fig. 1(a) are obtained. Next, the elements are transformed to the bandpass domain, and they are related to the specific technology used to design the filter.

The RN and NRN can be directly translated to distributed transmission lines as shown in Fig. 1(b). The RN consists of a unit capacitor in shunt configuration with a susceptance b. When this structure is moved to the other side of the inverter J_r, it becomes an inductance in series with a susceptance as detailed in [8]. This structure can be implemented with a classical $\lambda/4$ open-circuit transmission line at the frequency of the TZ, with the characteristic impedance being $Z_0 = 4\omega_0 L/\pi$ and L the equivalent inductance. On the other hand, the frequency and impedance scaling of the lowpass inductance is defined as,

$$L = \frac{Z_0}{2}\left(\frac{2\alpha + b_i}{J_{ri}^2 \omega_0}\right), \quad \alpha = \frac{f_0}{Bw} \tag{3}$$

with f_0 being the central frequency and Bw the bandwidth. Then, it is straightforward to compute the characteristic admittance of the $\lambda/4$ transmission line implementing the resonator as,

$$Y_{ri} = \frac{\pi}{4}\left(2\left(\frac{J_{ri}^2}{2\alpha + b_i}\right)\right) \tag{4}$$

The implementation of the NRN can be performed by means of an open-circuit (OC) or SC-stub depending on the sign of the reactance B_i. When the TZ is below the passband (negative in the lowpass domain) $B_i > 0$, while $B_i < 0$ when the TZ is above the passband [8]. Positive reactances will be implemented by means of an OC-stub, and negative reactances will be implemented using an SC-stub. Unlike the implementation of the resonator, the electrical length $\theta = \beta l$ can be freely chosen in the following way,

$$\begin{aligned} Y_{Bi} &= -jB_i \cot(\beta l) \quad B_i < 0 \\ Y_{Bi} &= jB_i \tan(\beta l) \quad\;\; B_i > 0 \end{aligned} \tag{5}$$

The concatenation of a shunt SC-stub with an admittance inverter and an SC-stub can be compacted into ACL sections [6, 7] as shown in Fig. 1(c). The TZs have to be set above the passband to obtain $B_i < 0$ (SC-stubs) in order to achieve such compactness. To carry out the equivalence, each NRN except the first and the last one will be split into two shunt NRNs with admittance $2Y_{Bi}$, so the filter will be finally composed of $(N-1)$ ACL sections.

3.1. Degree of Freedom in Asymmetric Coupled Lines

The equation in Equation (5) shows that there is a degree of freedom in the election of the electrical length of the SC-stubs. Among other considerations, this election will also affect the sensitivity of the filter. As seen in [6], the electrical length θ of the stubs will be directly related to the ACL section electrical length. On the other hand, it is well known that for a specific coupling value, shorter coupled lines will require a narrower gap while longer lines will require a wider gap. Since the coupling is a critical parameter in the design of the ACL, it is important to analyse how the coupling value deviates from the theoretical depending on variations in the electrical length θ or in the gap S. This can also be related to fabrication tolerances.

Although fabrication tolerances result in absolute variations, in this case, relative variations have been considered to carry out the analysis. Fig. 6 shows the relative deviation of the coupling value as a function of relative variation in the gap S (solid lines) and relative variation in the electrical length θ (dashed lines). Since the electrical length θ is set a-priori, three nominal cases have been considered for the analysis: $\theta = 30°$, $45°$, $60°$. It is seen that the shorter electrical length is less sensitive to changes on both the electrical length and the gap. Moreover, deviations in the electrical length lead to higher error in the coupling value than deviations in the gap.

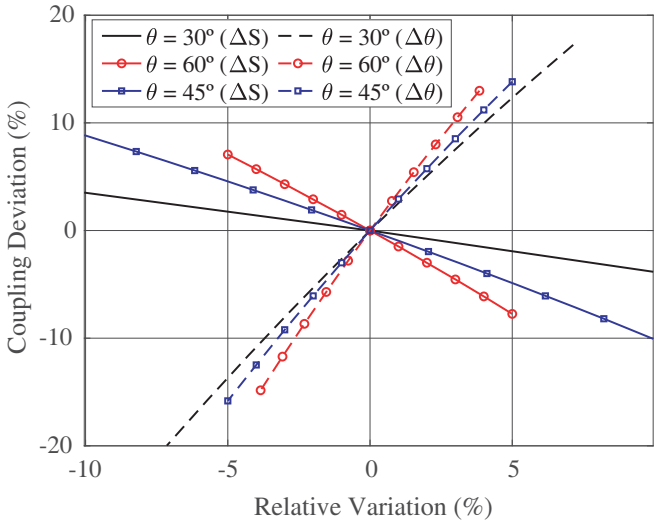

Figure 6. Relative deviation in the resulting coupling value as a function of relative variations of the gap S (solid lines) and electrical length θ (dashed lines) for coupled lines with $\theta = 30°$ (no symbol), $\theta = 45°$ (square) and $\theta = 60°$ (circle).

Taking into account the results in Fig. 6, it is desired to decrease, as much as possible, the electrical length θ of the ACL in the first/last section of the filter to minimize the effects of via-holes since they are mainly responsible for the in-band equiripple RL. The minimum θ value is set by the narrowest gap that can be implemented with the fabrication process.

4. EXPERIMENTAL VALIDATION

A prototype for the Ku-band in the range of 12,5 to 14,7 GHz has been developed to fulfill RL < -15 dB and OoB rejection higher than -40 dB at 9 and 17 GHz. The order of the filter is $N = 6$, and the RL

Table 1. Resulting valued for the lowpass prototype elements and corresponding admittances for the $\lambda/4$ resonators Y_{ri}, and short-circuited stubs Y_{Bi}.

	Res_1	Res_2	Res_3	Res_4	Res_5	Res_6
J_{ri}	2.753	4.180	4.954	4.685	4.420	2.604
b_i	−3.2	−3.7	−3.9	−3.9	−3.7	−3.2
B_i	−2.596	−5.079	−6.72	−6.009	−5.679	−2.629
Y_{ri} (Ω^{-1})	0.0261	0.0637	0.0916	0.0819	0.0712	0.0234
Y_{Bi} (Ω^{-1})	0.03	0.0587	0.0776	0.0694	0.0656	0.0304

Table 2. Obtained physical dimensions for the resonators of the fabricated prototype.

	Res_1	Res_2	Res_3	Res_4	Res_5	Res_6
W_r (μm)	140	120	120	120	120	140
L_r (μm)	1.5	1.54	1.09	1.09	1.54	1.5

Table 3. Obtained physical dimensions for the ACL sections of the fabricated prototype.

	ACL_1	ACL_2	ACL_3	ACL_4	ACL_5
W_a (μm)	120	60	130	60	120
W_b (μm)	40	110	140	110	40
L (μm)	560	1270	830	1270	565
S (μm)	10	40	140	40	10

Table 4. Comparison with other topologies based on Alumina substrates [2].

	FBW (%)	IL (dB)	RL (dB)	f_0 (GHz)	Group Delay (ns)	Size (mm)
CLF	28.6	1.5	13	14.21	0.2 ± 0.03	9×2
Hairpin	14.8	1.5	20	14.11	0.38 ± 0.04	10×6
Ring res.	9.7	2.2	17	14.38	0.64 ± 0.06	7×2.5
Interdigital	11.2	1.9	10	13.96	0.48 ± 0.03	3×3
This work	16.2	1.6	18	13.55	0.45 ± 0.05	7.9×3.9

has been set to −25 dB, so further degradation of the RL due to fabrication deviations can be accounted for. The allocation of the transmission zeros is $\Omega_i = [3.2, 3.7, 3.9, 3.9, 3.7, 3.2]$ rad/s, so the NRNs will be implemented by means of SC-stubs. With this distribution of finite transmission zeros, the selectivity mask is fulfilled as well as the out-of-band rejection. The resulting values for the lowpass prototype J_{ri}, b_i, and B_i from the synthesis procedure are stated in Table 4, as well as Y_{ri} and Y_{Bi} using Equations (4) and (5). The ratio between the central frequency f_0 and bandwidth Bw is $\alpha = 6.16$. The filter has been modelled in 3D using the Dey-Mittra conformal FDTD method described in [14] running on a GPU.

To reduce the sensitivity of the filter, the electrical lengths of the SC-stubs have been set for each section $\theta_i = [30°, 60°, 30°, 60°, 30°]$. As previously discussed, it is important to decrease, as much as possible, the electrical length in the first and last sections. The dimensions of the prototype for the resonators and the ACL sections are found in Tables 1 and 3, respectively.

The final prototype in Fig. 7 was fabricated in Alumina (10 mil) Al_2O_3 with $\epsilon_r = 9.6$, $\tan\delta = 0.0002$, $\sigma = 4.1e^7\ \text{Sm}^{-1}$. The via-holes are defined by a diameter of 150 μm in a square pad of $250 \times 250\ \mu\text{m}^2$ with a tolerance of ±50 μm in the positioning. This will affect effective lengths L_i of ACL sections.

The filter response is shown in Fig. 8 with IL = −1.6 dB, RL < −18 dB, and OoB higher than −50 dB at 9 GHz and 17 GHz as specified. Simulation and measurement show a very good agreement.

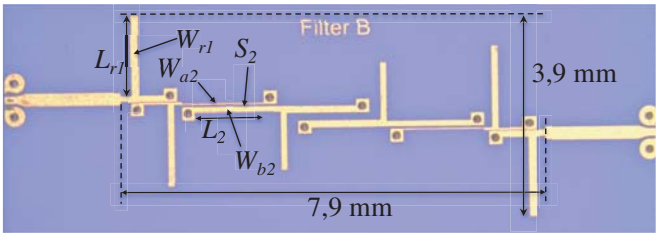

Figure 7. Fabricated in-line prototype using asymmetric coupled lines (ACL).

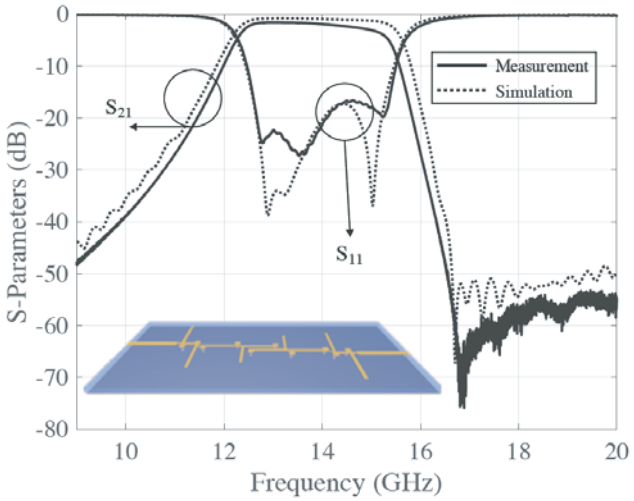

Figure 8. S-Parameters comparison between the EM simulation using CFTD (dotted line) and the measurement of the prototype (solid line).

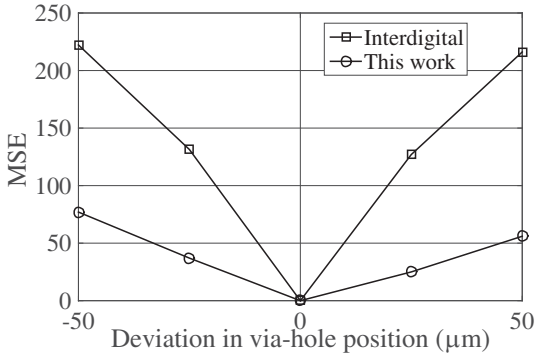

Figure 9. Comparison of the degradation on the RL as a function of the allocation of the via-holes between the proposed topology and the classical interdigital non fully-canonical configuration.

Deviations in the return losses are mainly due to the fabrication tolerances. As this was previously considered in the design process and the analysis of the worst case, the filter response fulfills return loss specifications. On the other hand, although the transmission zeros are expected to be more pronounced, coupling from input to output through the substrate could affect the filter response as discussed in [15]. The electrical performance comparison with other filter topologies based on Alumina substrate is found in Table 4. Although the aim of this work is to demonstrate the sensitivity improvement, it is evident that the obtained electrical performance is comparable with all-pole inline NFC conventional topologies based on coupled resonators.

Monte Carlo simulations have been carried out to analyze the degradation of the RL in the proposed design compared with an NFC inline interdigital filter. The minimum square error (MSE) has been calculated for the return losses degradation as a function of the absolute deviation of the positioning of the via-hole ground taking into consideration the fabrication tolerances, in this case, $\pm 50\,\mu$m. As seen in Fig. 9, the proposed design has a sensitivity around half of that of a conventional interdigital.

5. CONCLUSION

The analysis of the total expanded sensitivity has demonstrated that inline fully-canonical filters based on extracted pole sections are less sensitive than all-pole inline non-fully-canonical filters for even/odd topologies. The analysis has considered absolute variations in the main-line couplings, the most affected by fabrication tolerances, particularly variations in the positioning of the via-hole groundings. It has also been seen that, in the case of FC topologies, the allocation of the finite transmission zeros plays an

important role in the sensitivity. The closer the transmission zeros are to the bandpass, the faster the sensitivity drops in the transition region. However, at the same time, the distance between reflection zeros is higher leading to sensitivity increase in the in-band. With the aim to carry out the experimental validation, a Ku-band filter has been designed, simulated, fabricated, and characterized. The filter has been implemented in planar technologies by means of asymmetrical coupled lines. It has been shown experimentally to have a return loss sensitivity that approximates half of that of an equivalent interdigital filter, due to variations in the positioning of the via-hole groundings. The prototype presents IL $= -1.6$ dB, RL < -18 dB, and out-of-band rejection higher than -50 dB.

REFERENCES

1. Xu, J., W. Hong, H. Zhang, and H. Tang, "Compact bandpass filter with multiple coupling paths in limited space for Ku-band application," *IEEE Microw. Wirel. Co.*, Vol. 27, No. 3, 251–253, 2017.
2. Maasen, D., F. Rautschke, and G. Boeck, "Design and comparison of various coupled line Tx-filters for a Ku-band block upconverter," *German Microwave Conference (GeMiC)*, 225–228, 20016.
3. Goldfarb, M. E. and R. A. Pucel, "Modeling via hole grounds in microstrip," *IEEE Microwave and Guided Wave Letters*, Vol. 1, No. 6, 135–137, 1991.
4. Swanson, D. G., "Grounding microstrip lines with via holes," *IEEE Trans. Microw. Theory Tech.*, Vol. 40, No. 8, 1719–1721, 1992.
5. Yang, Y., M. Yu, and Q. Wu, "Advanced synthesis technique for unified extracted pole filters," *IEEE Trans. Microw. Theory Tech.*, Vol. 64, No. 12, 4463–4472, 2016.
6. Park, J., S. Lee, and Y. Lee, "Extremely miniaturized bandpass filters based on asymmetric coupled lines with equal reactance," *IEEE Trans. Microw. Theory Tech.*, Vol. 60, No. 2, 261–269, 2012.
7. He, Y., G. Wang, X. Song, and L. Sun, "A coupling matrix and admittance function synthesis for mixed topology filters," *IEEE Trans. Microw. Theory Tech.*, Vol. 64, No. 12, 4444–4454, 2016.
8. Giménez, A., J. Verdú, and P. de Paco, "General synthesis methodology for the design of acoustic wave ladder filters and duplexers," *IEEE Access*, Vol. 6, 47969–47969, 2018.
9. Cameron, R., C. Kudsia, and R. Mansour, *Microwave Filters for Communications Systems: Fundamentals, Design, and Applications*, Wiley, 2018.
10. Macchiarella, G., "Accurate synthesis of inline prototype filters using cascaded triplet and quadruplet sections," *IEEE Trans. Microw. Theory Tech.*, Vol. 50, No. 7, 1779–1783, 2002.
11. Martínez-Mendoza, M., C. Ernst, J. A. Lorente, A. Álvarez-Melcón, and F. Seyfert, "On the relation between stored energy and fabrication tolerances in microwave filters," *IEEE Trans. Microw. Theory Tech.*, Vol. 60, No. 7, 2131–2141, 2012.
12. Martínez-Mendoza, M., F. Seyfert, C. Ernst, and A. Álvarez-Melcón, "Formal expression of sensitivity and energy relationship in the context of the coupling matrix," *IEEE Trans. Microw. Theory Tech.*, Vol. 60, No. 11, 3369–3375, 2012.
13. Nedelchev, M. and D. Dobrev, "Low sensitivity symmetrical response microwave filters, *Microelectronics Journal*, No. 37, 546–553, 2006.
14. Junkin, G.. "Conformal FDTD modeling of imperfect conductors at millimeter wave bands," *IEEE Trans. Antennas Propag.*, Vol. 59, No. 1, 199–205, 2011.
15. Triano, A., J. Verdú, P. De Paco, T. Bauer, and K. Wagner, "Relation between electromagnetic coupling effects and network synthesis for AW ladder type filters," *IEEE International Ultrasonics Symposium (IUS)*, 2017.